

Chapter 3

In-situ Measurements of Aerosols from the High-Altitude Location in the Central Himalayas



Hema Joshi, Manish Naja and Tarun Gupta

Abstract Aerosols, both natural and anthropogenic, affect the Earth's climate directly due to the absorption and scattering of solar radiation and indirectly by modifying the cloud microphysics. Due to the short lifetime of these aerosols, their distribution is non-uniform and large uncertainties exist in their estimates at global and regional scale. The characteristics of atmospheric aerosols vary largely from one region to another due to spatial and temporal variations in the emission sources, transport, atmospheric transformation and removal of aerosol particles. The aerosol measurements over the Himalayan region are of crucial importance in order to provide a far-field picture quite away from potential sources. The ground-based measurements of aerosols are utilized along with satellite data to explain various aerosol characteristics over the Himalayan region. The roles of different processes such as boundary layer dynamics, meteorology, regional and long-range transport are assessed. In addition, the aerosol variation over the foothills of the Himalayas in the Indo-Gangetic Plain region has also been studied and the role of the boundary layer dynamics and updraft/downdraft of aerosols is elaborated. The high-altitude location of Himalayas is characterized by the low aerosol loading specially in winter, while significant aerosol abundance is observed in the spring. However, the significant aerosol abundance is observed over the foothills location throughout the year. The strong confinement of aerosols in the foothill region is evident, which leads to the significant enhancement in the surface concentration of aerosols. Interestingly, in the spring season, significant aerosol abundance is seen over the Himalayan region as well. The investigation of the mixing layer depth and the vertical distribution of aerosols over this region in spring reveals the transport and buildup of aerosols from the foothills region to the Himalayan region. The role of absorbing aerosols in the radiation budget over the central Himalaya region is also discussed.

H. Joshi (✉) · T. Gupta
Indian Institute of Technology, Kanpur 208016, Uttar Pradesh, India
e-mail: joshihm@iitk.ac.in

M. Naja
Aryabhata Research Institute of Observational Sciences, Nainital 263001,
Uttarakhand, India

Keywords Aerosol optical depth · Black carbon · Mixing layer depth · Vertical distribution · Himalayas · Indo-Gangetic Plain

3.1 Introduction

The global climate system depends upon the balance between the incoming solar radiation and outgoing long-wave (infrared) terrestrial radiation (Charlson et al. 1991; Hansen et al. 1998; Seinfeld et al. 2004) and an interaction between its subcomponents. The changes in the aerosol content and greenhouse gases present in atmosphere alters the radiative balance of the climate system (Haywood and Ramaswamy 1998; Myhre et al. 1998). The quantification of radiative forcing by aerosols is more complicated and uncertain than greenhouse gases due to high variability in aerosol mass and particle number concentrations in space and time owing to their short lifetime (about a week) as compared to the greenhouse gases (which have longer lifetime). Aerosols are known to affect the radiation budget through direct effect (through scattering and absorption of the incoming radiation) and indirect effect (modification of the microphysical properties of clouds). Aerosols thus have substantial influence on the Earth climate at the regional and global scales by affecting the radiation budget, cloud microphysics, hydrological cycle, and monsoon patterns (Lelieveld et al. 2001; Jacobson 2001). Interestingly, the aerosols of anthropogenic origins are found to be associated with the climate change via their interaction with radiation and clouds (Boucher et al. 2013).

The lack of observations of aerosols characteristics and spatio-temporal distribution coupled with the multi-faceted impacts on climate makes aerosols one of the least understood components of the Earth's climate (IPCC 2007; Boucher et al. 2013). There exist large uncertainties in their global and regional estimates (Ramanathan et al. 2001a) due to non-uniform distribution over the globe. Although the model predictions have significantly improved in recent times, still the most of the available models possess high degree of uncertainty associated with their use and capturing the actual magnitude of aerosol. The ground based actual measurements of aerosols and their properties thus are of crucial importance for realistic impact assessments and model evaluations.

Some of the recent studies have indicated the significant aerosol abundance over the South Asian region (Ramanathan et al. 2001b; Lelieveld et al. 2001) and the possible impacts of aerosols. This region is also marked with the high levels of absorbing aerosols (Koch and Hansen 2005; Lawrence and Lelieveld 2010). In recent times, the increase in anthropogenic activity has been witnessed in terms of accelerated population density, industrialization and urbanization leading to aerosol abundance in the atmosphere. The enhancement in the aerosol emission is reported over the Asian region (Zhang and Reid 2010; Lu et al. 2012; Boucher et al. 2013) including the Indian region (Porch et al. 2007; Streets et al. 2009; Moorthy et al. 2013a). The Indo-Gangetic Plain (IGP) region is marked with the high abundance of aerosol and gaseous pollutants throughout the year, which not only affects significant pollution

load over this region (Dey et al. 2004; Singh et al. 2004; Gautam et al. 2010, 2011; Giles et al. 2011; Joshi et al. 2016), but also the nearby elevated slopes of Himalayas (Pant et al. 2006; Dumka et al. 2010; Gobbi et al. 2010; Bonasoni et al. 2010; Marinoni et al. 2010; Kumar et al. 2011; Srivastava et al. 2012). Aerosols from IGP can be transported to high altitude regions by enhanced convection and uplifting, and can have myriads of effects, once reached the Himalayas. The close association between the pollution load of IGP is found to be associated to the Himalayan climate, which thereafter affects the regional climate significantly by affecting the dynamics, hydrological cycle and radiation budget of the region (Menon et al. 2002; Lau and Kim 2006; Lau et al. 2010).

3.1.1 Atmospheric Aerosols

Atmospheric aerosols are defined as particles in solid, liquid or in mixed phase dispersed in the atmosphere (Seinfeld and Pandis 1998). The term aerosol was coined in the year 1918 by the physical chemist E. G. Donnan. It was considered as analogous to the term hydrosol, which is a stable liquid suspension of solid particles (Hinds 1999). A. Schmauss got the term integrated into the meteorological literature in the early 1920s. Atmospheric aerosols are two/three-phase systems (solid-gas, liquid-gas and a combination of both), the common examples of which are dust, fume, smoke, fog, haze, smoke, smog and clouds (Seinfeld and Pandis 1998). The size of aerosols varies from $\sim 10^{-3}$ to 100 μm (Junge 1963; Prospero et al. 1983).

3.1.2 Aerosol Sources and Production

Atmospheric aerosols can be of natural as well as of anthropogenic origin (Seinfeld and Pandis 1998) (Fig. 3.1). The natural sources include windborne dust, sea spray, volcanic activities and biomass burning, while anthropogenic activities mainly include fuel combustion, industrial emissions, transportation and biomass burning due to crop harvest. There are also common sources i.e., biomass burning, soil dust emissions etc., which can be originated from both the natural and anthropogenic sources. The natural aerosols are reported to be present in the higher amount $\sim 4\text{--}5$ times larger than anthropogenic ones on the global scale, but regional variations in anthropogenic aerosols are reported to change this ratio significantly in the industrialized Northern Hemisphere (Seinfeld and Pandis 1998). Aerosols, when directly emitted from their sources are called primary aerosols (e.g., black carbon, soil dust, sea salt). Aerosols can also be formed in atmosphere by the oxidation of the precursor gases (i.e., nitrogen oxides, sulphur dioxide, and volatile organic compounds), the resultant oxidation product then nucleate to form new particles or condense on pre-existing ones forming secondary aerosols (Seinfeld and Pandis 1998).

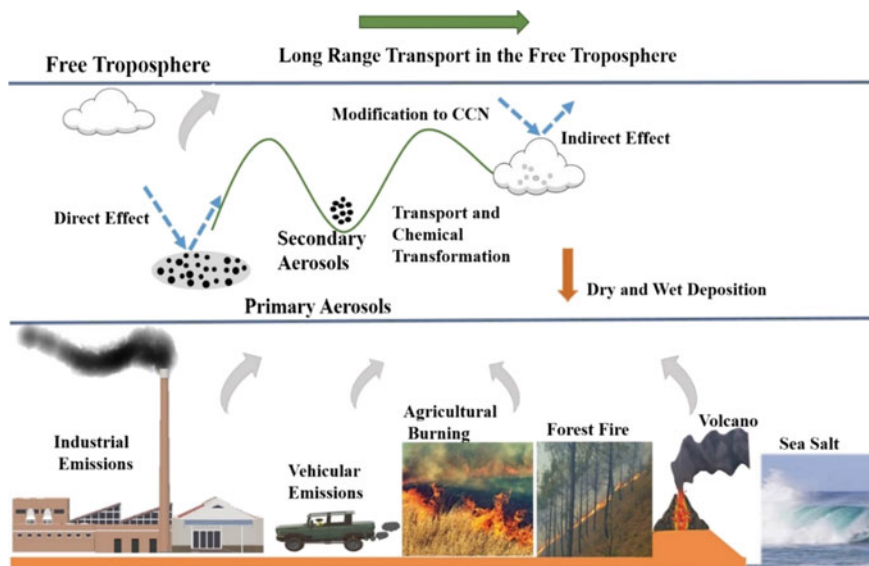


Fig. 3.1 Schematic representation of aerosol emission sources, deposition, transport and transformation processes, and aerosol effects (direct and indirect)

Aerosols are mainly produced by bulk to particle conversion process also called as “mechanical disintegration”, which is the most common and major process of aerosol production (Prospero et al. 1983). The gas-to-particle production of aerosols however is a secondary process of aerosol production. The aerosols formation occurs as a result of chemical reactions between various gaseous species in the atmosphere, followed by nucleation and condensation. The gases or vapors with low vapor pressure in the atmosphere condense on to existing particles and increase the mass of aerosols or condense to form new particles in the air. The particles produced from gas-to-particle process are hygroscopic in nature and are efficient cloud condensation nuclei (CCN). Atmospheric aerosols are broadly classified in two main categories, fine and coarse mode aerosols (Fig. 3.2). The fine fraction of aerosols is comprised of the Aitken mode and the accumulation mode of particles. The particles in the accumulation mode are of crucial importance as they are most stable, characterized by larger lifetime and have the significantly high impact on climate. The most common types of the aerosols found in the atmosphere are mentioned below.

3.1.2.1 Dust Aerosols

Dust aerosols are one of the major type of natural aerosols (Alfaro et al. 1997) originated predominantly from desert regions in the Northern Hemisphere. The dust source regions mainly include deserts, semi-arid desert fringes, dry lakebeds, and the arid regions with low vegetation. The origin of dust can be both the natural as

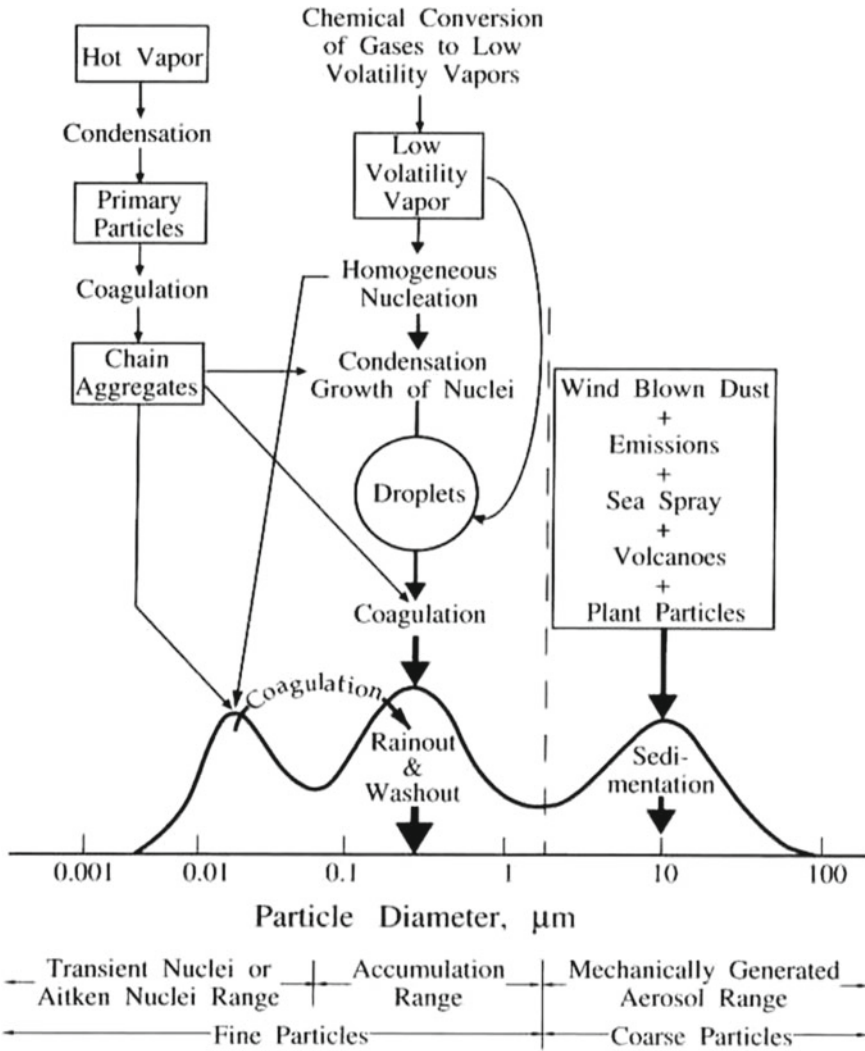


Fig. 3.2 Idealized representation of the size distribution (surface area) of the atmospheric aerosol (Whitby 1978). The common formation mechanism, sources and removal processes of aerosol are shown

well as anthropogenic in origin. The larger size dust particles are found near the source regions while the small size dust can easily transport to much larger distances (Prospero et al. 2002).

3.1.2.2 Sea Salt

Sea salt aerosols are of natural origin contributing to about ~30% of global aerosol burden (Fitzgerald 1991). These aerosols are generated by a wide range of physical processes, the most effective of which is bursting of air bubbles entrained in the ocean surface during white cap formation (Blanchard 1985; Monahan 1986), which strongly depends upon the wind speed. These aerosols are hygroscopic in nature and are very efficient cloud condensation nuclei (CCN).

3.1.2.3 Black Carbon

Black carbon also called as 'BC' is the most absorbing primary aerosol with strong and wide absorption in the visible and Infrared (IR) range. It is emitted from the incomplete combustion processes such as fossil fuel and biomass burning, thus much of the atmospheric BC is of anthropogenic origin. BC is known to retain its basic form at very high temperatures, with a vaporization temperature near 4000 K (Bond et al. 2013). It serves as an excellent tracer (due to its inert nature and longer lifetime) to study the anthropogenic influence at remote sites. BC can undergo the regional and intercontinental transport even to the remote and clean locations in Arctic (Stohl 2006).

3.1.2.4 Organic Carbon

Organic carbon (OC) is produced from both primary emissions as well as secondary transformations. The OC aerosols scatter the solar radiation and are known as scattering aerosols. OC aerosols are comprised of myriads of organic compounds with varying volatility and polarity, which makes the study of the effect of individual organic compounds quite challenging. Due to the presence of polar functional groups, for example carboxylic and dicarboxylic acids, OC aerosols also participate in cloud droplet nucleation (Saxena and Hildemann 1996).

3.1.2.5 Sulphate and Nitrate Aerosols

Sulphate aerosols are produced via chemical reactions in the atmosphere from gaseous precursors (i.e., SO₂ from anthropogenic sources and volcanoes, and dimethyl sulphide (DMS) from biogenic sources, especially marine planktons) and are efficient CCN. The volcanic eruption also adds large amount of SO₂ into the

stratosphere, where it is converted to sulphate aerosols. The industrial activities also contribute to sulphate aerosols (Charlson et al. 1992). Nitrate aerosols are also produced by chemical reactions in the atmosphere from gaseous precursors, produced either naturally or anthropogenically and are also efficient CCN.

3.1.3 Aerosol Transport, Transformation and Removal

Atmospheric aerosols, once airborne can undergo the change in their size and composition by coagulation with other species, condensation of vapor, by evaporation, chemical reactions, and by activation in presence of water supersaturation to form clouds and fog. Atmospheric aerosols can also exist in different mixing state (externally or internally) depending upon how the constituent chemicals are distributed among the particles. The particles from diverse sources remain separated in an external mixture, while diverse chemical components get mixed to form a single particle in an internally mixed aerosols. The nature of mixing affects optical and physical properties of aerosols, and plays a crucial role in the aerosol radiative forcing. The changes in the aerosols number density, size distribution and hence in their optical and radiative properties can also occur during the transformation process. The main aerosol transformation processes are known to be condensational growth, coagulation, and the processing of aerosols by non-precipitating cloud cycling. The transformation processes are not the removal process as aerosol mass is not removed from the atmosphere during this process.

Aerosols are known to be removed from the atmosphere by two main processes: dry and wet removal processes. The dry removal processes, also called as dry deposition or sedimentation, involves sedimentation of particles due to gravity and impaction onto surfaces, while the wet processes involve the rain out and wash out processes (Pruppacher and Klett 1978). The sedimentation process is significant only for aerosols with diameters greater than a few micrometers. Wet removal however is the main removal process for smaller particles. The wash out scavenging is the below cloud scavenging and involves removal of aerosols from the atmosphere by the falling rain drops. The rainout process mainly describes the removal of a cloud condensation nuclei and takes place within the cloud. Aerosols also undergo transport at regional, intercontinental and global scales from their source region to distant locations by means of prevailing winds. The synoptic scale air masses influence the aerosol concentration significantly (Smirnov et al. 1995). Aerosols when get transported to the free troposphere, can stay there for a longer time and can undergo long range transport from there.

3.1.4 Brief Background and the Study Region

The systematic measurements of aerosols have been initiated over the Indian region since the 1980s at several distinct geographical regions under I-MAP (Indian Middle Atmosphere Programme) and ISRO-GBP (Indian Space Research Organization, Geosphere Biosphere Programme) (Moorthy et al. 1999). Several campaigns were also conducted i.e., The Indian Ocean Experiment (INDOEX) (Satheesh and Ramanathan 2000; Ramanathan et al. 2001b), Integrated Campaign for Aerosols, gases and Radiation Budget (ICARB) (Moorthy et al. 2008), and other land campaigns (LC-I, LC-II) in order to better understand the role of aerosols over various regions (mainland and oceans). The initiation of establishing several permanent aerosol monitoring stations from the ground based diverse locations started under Aerosol Radiative Forcing over India (ARFI) project of ISRO-GBP. Initially few monitoring stations were established, followed by more over the time in order to study aerosol impacts, to generate regional aerosol database, and radiative forcing maps for climate impact assessment over the Indian region. Realizing the importance of the aerosol measurements from the Himalayan region, aerosols observations were initiated at the high-altitude site, Aryabhata Research Institute of Observational Sciences (ARIES) (earlier known as state observatory) (29.4° N, 79.5° E, 1958 m msl), Nainital in year 2002 under the ISRO-GBP program. The actual ground-based observations of aerosols are quite limited and nearly non-existing over the Himalayas considering the diversity of the region and topographic changes. In the later years, aerosols observations were also setup at Kullu (31.9° N, 77.1° E, 1154 m msl) (since year 2007), and more recently at Hanle (32.7° N, 78.9° E, 4520 m msl) (since year 2009).

Aerosol observation and reported studies from Nainital site had shown that the site is characterized by very low aerosol optical depth (AOD) comparable to the Antarctic environment in winter, while in summer typical to the continental location (Sagar et al. 2004). The observations of black carbon mass concentration however (started later in November 2004 at the site) indicated that the BC contributes about $\sim 5.0\%$ to the composite aerosol mass at the site in the winter season (Pant et al. 2006). The site also experiences the dust storm, which typically originates from the Thar Desert. The enhancement in the aerosol columnar loading due to the dust storm was reported to be two to four times higher particularly at longer wavelengths (Hegde et al. 2007). Aerosol optical and physical properties and surface concentration of BC was studied and reported from the site (Dumka et al. 2008, 2010). The possibility of influence of the aerosols from the nearby valley region to the observation site was also indicated, however the actual simultaneous observations at the foothills locations were not present for the comparison. Aerosol observation of BC mass concentration was then initiated at the low altitude foothills site, Pantnagar (29.0° N, 79.5° E, 231 m msl) (since year 2009) in the Indo-Gangetic Plain region in order to study the aerosol sources, the role of boundary layer dynamics and updraft/downdraft of aerosols from IGP region to the nearby Himalayan region.

In the present study, an attempt has been made to study the aerosol climatology from the high-altitude site in the central Himalayan region. The long-term datasets of aerosols have been utilized for the trend estimations in aerosols over this region. Further, aerosol characterization from foothills location in the Indo-Gangetic Plain region has also been made and reported and the associated processes have been discussed. The possible sources of aerosols, their seasonality and processes governing the observed concentration or loading have been discussed. The columnar, surface and vertical variation of aerosols have been studied and discussed here along with the aerosol measurement from the space borne sensors. These ground-based datasets have also been utilized for the comparison with the model simulations over this region.

3.2 Measurement Sites, Observations and Database

The ground-based observations of aerosols have been used from a high altitude, regional representative site, Nainital (29.4° N, 79.5° E, 1958 m msl) (Fig. 3.3) in the central Himalayas. It is an ideal site for studying the far-field impact of anthropogenic aerosols, by virtue of being situated far away from the major aerosol sources. In addition, aerosol observations from the low altitude, foothill site, Pantnagar (29.0° N, 79.5° E, 231 m msl) in the Indo-Gangetic Plain (IGP) region has also been used (Fig. 3.3), which represents as an ideal site for studying the aerosol characteristic near the source region. Although, these two sites are located at an aerial distance of ~ 30 km, they are characterized by different topography, vegetation type and meteorological parameters. The site, Nainital is located at the mountain top, the north and north-east of which is the high-altitude Himalayan

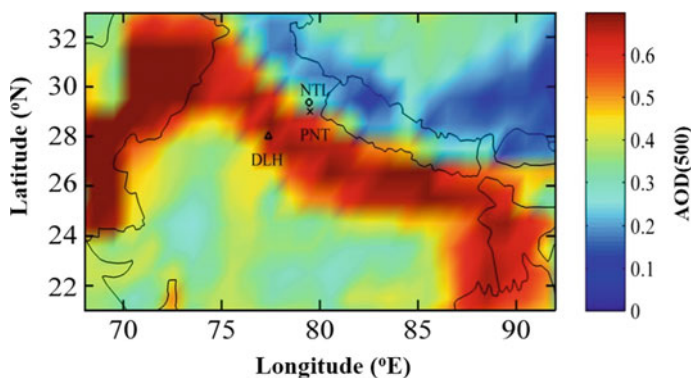


Fig. 3.3 Spatial variation of aerosol optical depth (AOD 550 nm) obtained from MODIS (Terra) satellite. The location of the high-altitude observation site, Nainital (NTL: 29.4° N, 79.5° E, 1958 m msl) in the central Himalayas and the foothill site, Pantnagar (PNT: 29.0° N, 79.5° E, 231 m msl) in the Indo Gangetic Plain region is shown. The country capital Delhi (DLH) is also shown

mountain range, while towards the south and southwest lies the low altitude plain merging with the IGP region. The mean temperature experienced at the Nainital site reaches maximum ~ 22.3 °C ($T_{\max} \sim 30$ °C) in June, while minimum monthly mean in January is ~ 5.2 °C ($T_{\min} \leq 0$), while at Pantnagar site, the maximum monthly mean temperature observed in June reaches ~ 30 °C ($T_{\max} \sim 42$ °C), with minimum in January is ~ 10 °C ($T_{\min} \geq 3$ °C) (Joshi et al. 2016). The additional details regarding the present high-altitude site have been reported in the earlier studies (Pant et al. 2006; Dumka et al. 2010; Naja et al. 2016).

The measurements of black carbon (BC) mass concentration has been made using the optical measurements from seven-channel (0.37–0.95 μm) Aethalometer (Magee Scientific, USA). The light attenuation through a quartz filter paper has been measured in order to compute the absorption coefficients by measuring the light transmission through the particle laden and particle free reference spot of filter. The absorption coefficients were then converted into the BC mass concentration by utilizing the calibration factors of corresponding wavelengths as mentioned by manufacturer (Hansen et al. 1984). This instrument utilizes the 0.88 μm wavelength for determination of BC mass concentration. BC is reported to be the principal absorber of light at this wavelength (Bodhaine 1995) with negligible contribution from other components. BC measurements at 0.88 μm from Aethalometer has been extensively used in literature (Hansen et al. 1984; Moorthy et al. 2004; Pant et al. 2006; Satheesh et al. 2008 and many others). Although the optical attenuation technique used in this instrument is widely used, it is found to suffer from various systematic errors as being the filter-based absorption technique and needs to be corrected. The instrument suffers from the uncertainty arising due to the multiple scattering in the quartz fibre matrix of the tape (also called C-factor) and another for ‘shadowing effects’, arising due to deposition of scattering material along with BC in filter tape, which needs to be corrected (Weingartner et al. 2003). Additional details regarding instrumentation, methodology and associated uncertainty are quite well documented (Hansen et al. 1984). The details of the instrument setup can be found in Pant et al. (2006) and Dumka et al. (2010).

The columnar abundance of aerosols has been studied using the hand held, Sun-photometer MICROTOPS-II (Solar Light Company, USA), a very popular and widely used instrument for measuring the aerosol optical depth. The instrument contains five different interference filters at 380, 440, 500, 675 and 870 nm wavelengths, and provides aerosol optical depth (AOD) corresponding to these channels using Bouguer-Lambert-Beer law. The instrument is equipped with accurately aligned optical collimators, with a full field view of 2.5° . Instrument is integrated with the internal baffles, which eliminate internal reflections. The filter used in the 380 nm channel has the wavelength precision of ± 0.4 nm, and a full width at half maximum (FWHM) band pass of 4 nm, while other channels are characterized by peak wavelength precision of ± 1.5 nm, and FWHM band pass of 10 nm. The instrument is operated only when the region of sky ($\sim 10^\circ$) around the Sun is free from clouds in order to avoid cloud contamination in the data (Pant et al. 2006). The details of the instrument have been well documented (Morys et al. 2001; Ichoku et al. 2002). The instrument setup at the site has been same as described in Pant et al. (2006) and Kumar et al. (2011). AOD

observations at the foothills region have been studied using data from AERONET (Aerosol Robotic NETwork) (Holben et al. 1998, 2001). The direct Sun and diffuse sky radiances at eight spectral channels (340, 380, 440, 500, 675, 870, 940, and 1020 nm) are measured from the CIMEL sun/sky radiometer of AERONET (Holben et al. 2001; Eck et al. 1999). The direct Sun measurements were made once every 15 min at 340, 380, 440, 500, 675, 870, 940, and 1020 nm. The uncertainty in AOD retrieval under cloud free conditions is less than less than ± 0.02 for shorter wavelengths and ± 0.01 for $\lambda > 440$ nm. The quality assured datasets which are pre and post field calibrated, cloud cleared and manually inspected were used.

The vertical variation of aerosols has been studied using the Cloud-Aerosol Lidar and Infrared Pathfinder Satellite Observation (CALIPSO) (Winker et al. 2009) datasets. CALIPSO was launched in April 2006 in the A-train constellation of satellites (Stephens et al. 2002) as part of the NASA Earth System Science Pathfinder (ESSP) program in collaboration with the French space agency CNES. The main aim of CALIPSO was to understand and fill the existing gaps in the global distribution and properties of aerosols and clouds. The satellites of the A-train are in a 705 km sun synchronous polar orbit, with a 16-day repeat cycle characterized by an equatorial passing time of about 13:30 local solar time. CALIOP is the first polarization lidar to provide global atmospheric measurements of aerosol and clouds around a solid-state Nd:YAG laser, which produces simultaneous, coaligned, pulses at 1064 and 532 nm. The elastic backscatter observations are utilized at 532 and 1064 nm channels (Winker et al. 2009). The CALIPSO profiles of aerosol extinction coefficient (version-3, 5-km horizontal resolution datasets) have been studied. The Hybrid Extinction Retrieval Algorithm (HERA; Young and Vaughan 2009) has been used to derive the extinction coefficients. The six aerosol types are represented by aerosol models with a prescribed bi-modal size distribution (fine and coarse mode) and a characteristic complex refractive index for each mode and wavelength (Omar et al. 2009). The discrimination between ice clouds and water clouds and the identification of non-spherical aerosol particles is done by depolarization measurements. Additionally, the other information like the aerosol size and type of aerosols as smoke, dust, polluted dust etc. has also been obtained from the ratios of the signals obtained at the two wavelengths.

The model simulations have also been used in order to evaluate the model performance over the region. The Weather Research and Forecasting Model (version 3.6) (Skamarock et al. 2008) coupled with chemistry (Grell et al. 2005) has been used to simulate BC mass concentration. In order to avoid influence due to topography, the observations from the low altitude site, Pantnagar has been compared. The model domain has been centered at Pantnagar (79.5° E, 29.0° N) and has (100, 100, 37) grid points in (longitude, latitude, vertical) directions. Aerosol processes have been taken from GOCART bulk aerosol scheme (Chin et al. 2002). Anthropogenic emissions of BC, OC and SO₂, PM_{2.5} and PM₁₀ have been taken from Emission Database for Global Atmospheric Research (EDGAR) available at a spatial resolution of 0.1° × 0.1° (Janssens-Maenhout et al. 2012). The complete model setup and other details have been reported in Kumar et al. (2012) and Joshi et al. (2016).

3.3 Aerosols Climatology and Trends from a High-Altitude Site

The high-altitude regions of Himalayas are far away from any major anthropogenic activities and are best suited to study the regional enhancement in aerosols and its impacts. The long-term ground-based datasets of aerosol black carbon (2005–2016) and aerosol optical depth (2005–2014) from the regional representative site, Nainital in the central Himalayas, has been utilized to infer aerosol climatology and trends in aerosols over this region. The ground-based estimation of aerosol trends over the Himalayan region are of crucial importance considering the complex topography of the region, limited availability of observations and close proximity of the Himalayan region from the highly polluted Indo Gangetic Plain (IGP) region.

The climatology in BC was examined. The minimum BC concentration was observed during the July–August due to scavenging during monsoon, while high BC was observed from March till May season each year. The monthly mean BC concentration during the observation period showed as high as $\sim 2.49 \mu\text{g m}^{-3}$ in April month, while monthly BC as low as $\sim 0.29 \mu\text{g m}^{-3}$ was observed in September month. The influence of the background level enhancement in the BC has been explored by examining the daytime and the nighttime levels in BC. As the site is located at the mountain top surrounded by the valley region, so the diurnal variations in BC are indicative of the evolution of the aerosols from nearby valley regions and other low altitude regions to the site. The amplitude in BC has been found to be maximum in winter season, while nearly flat pattern in BC was observed in spring. The close examination of data reveals that during winter (December to February) the background (night time) levels of BC were quite low, while BC during daytime showed a significant enhancement due to transport of BC from nearby valley regions to this site. The major contribution of BC in winter has been observed to be coming from the valley regions during the daytime, while during nighttime, BC aerosols along with other aerosols subside in the valley region. Quite interestingly, significant enhancement in background (night time) BC is seen in the spring (March to May) each year due to the biomass burning around the nearby regions. The long-term data of BC were then utilized for examining the trend over this region. The linear trends were estimated in the monthly mean BC, which shows a positive slope of ~ 1.511 (ng m^{-3} per year) with standard error (σ_w) of ~ 0.975 . The positive slope in BC indicates that the black carbon aerosols have been increasing at the site although at a slow rate. The reported BC trends are very less and nearly non-existing over the Indian region, specially over the Himalayan region. The observed trends might be useful to study the actual impact of aerosols over this region in future. The observed increasing trends in BC were consistent with some of the reported model based studies, which had reported increased warming, accompanied by earlier snow melt and retreat of high mountain glaciers over the Himalayas (Jain 2008; Kulkarni et al. 2007) and Tibetan Plateau (TP) regions (Ramanathan et al. 2007; Flanner et al. 2009; Menon et al. 2010). Based on the back trajectory analysis, Lu et al. (2012) also reported that the amount of BC received by the Himalayas and Tibetan Plateau (HTP) region

has increased by 41% from 1996 to 2010, the main contributing source regions were reported to be South Asia and East Asia accounting for 67 and 17% of BC transported to the HTP on an annual basis.

In addition, the climatology in the columnar abundance of aerosols was examined, which revealed that the climatological daily mean AOD (500 nm) varied from 0.019 (January) to 0.820 (April) while monthly mean climatological mean AOD was found to vary from ~ 0.189 to ~ 0.515 , with an annual mean ~ 0.189 (500 nm). The aerosol loading was found to be minimum in winter and maximum in spring season at Nainital. It is interesting that minimum AOD does not occur in the monsoon because of the hygroscopic growth of aerosols, but happens in winter. The enhancement in the aerosol due to the northern Indian biomass burning was reported at the site in spring season. The enhancement in the BC and AOD (0.5 mm) due to biomass burning was found to be $\sim 1.8 \mu\text{g m}^{-3}$ ($\sim 145\%$) and 0.3 ($\sim 150\%$) respectively at the site, leading to the additional atmospheric warming of 19 W m^{-2} , with the enhancement in the lower atmospheric heating rate by 0.8 K day^{-1} (Kumar et al. 2011). The northern Indian region experiences the influence of the dust transported from the northwestern arid regions to the IGP (Prospero et al. 2002; Agnihotri et al. 2011) in each spring (Sikka 1997; Dey et al. 2004). The influence of the transported dust from Thar Desert has been reported at the Nainital site (Hegde et al. 2007). Dust, when mixed with BC, is reported to cause enhanced absorption even greater than what is observed solely due to BC in IGP (Gautam et al. 2011).

AOD at the site also showed increasing trend. The monthly mean AOD data (500 nm) when examined for trend showed a positive slope of $\sim 0.000774 \text{ year}^{-1}$ with a standard error (σ_ω) of ~ 0.000415 . The multi-wavelength data of AOD was used to examine the aerosol size by investigating the 'angstrom exponent' (AE) by the method mentioned by Angstrom (1964). The slope of the monthly mean AE (440–870 nm) was found positive $\sim 0.00374 \text{ year}^{-1}$ with a standard error (σ_ω) of ~ 0.00144 . The increasing trends, observed over the site, indicate that the aerosol loading might have increased over the site in the recent times. The observed increase in the aerosol loading is in accordance to what is reported at the other locations, where AOD is reported to increase. Over the Indian region, Moorthy et al. (2013a) had utilized the AOD data of various ground-based networks of observatories (under ARFI project of Indian Space Research Organization) to deduce the regional nature of aerosol loading over this region. It was reported that AOD over the Indian region increased at a rate of 2.3% (of its value in 1985) per year, while more rapidly with enhancement of $\sim 4\%$ in the recent decade (Moorthy et al. 2013a). The major fraction of this enhancement was also found to be of anthropogenic origin.

The observed trends at the present site ($\sim 0.0007 \text{ year}^{-1}$) have been compared with the AOD trends reported by Babu et al. (2013). The observed trends at the present site were less (as the site is situated far away from any major anthropogenic source region) than what reported at Port Blair (an island location in the Bay of Bengal) $\sim 0.0097 \text{ year}^{-1}$, and Minicoy (location in Indian Ocean) $\sim 0.0208 \text{ year}^{-1}$, Trivandrum (a coastal location in south India) $\sim 0.011 \text{ year}^{-1}$, Visakhapatnam (industrialized coastal location in east coast of India) $\sim 0.0266 \text{ year}^{-1}$, Hyderabad (Industrialized, urban location close to central India) $\sim 0.0127 \text{ year}^{-1}$, and Dibrugarh (North-Eastern

India) $\sim 0.0135 \text{ year}^{-1}$. Interestingly, AOD trend over the two nearby IGP locations Patiala (semi urban, western part of Northern India) and Kanpur (Industrialized, urban location in IGP) were also found to be increasing at a rate of $\sim 0.0127 \text{ year}^{-1}$ and $\sim 0.0089 \text{ year}^{-1}$ respectively. The increased aerosol abundance at these two IGP locations indicated that there is a possibility of the regional level enhancement of aerosols over the IGP region, which might lead to the background levels enhancement of aerosols at nearby Himalayan regions in future. The combined effect of the observed enhanced aerosol loading and BC over this region indicates the possibility of enhanced atmospheric warming over this region in future as well. The atmospheric warming strongly depends upon the contribution of absorbing aerosols. The increasing trend in aerosol loading with increasing trend in BC contributes to the net warming, while decreasing trend in BC suggests decreased warming or less warming potential of aerosols.

3.4 Aerosol Variation at the Adjacent Foothills Location

In order to see the aerosol variation near the source region in the foothill locations in IGP region and its influence to the nearby Himalayas, the aerosol measurements were initiated at the foothills location, Pantnagar (29.0° N , 79.5° E , 231 m amsl) shown in Fig. 3.3. BC serves as an excellent tracer of anthropogenic influence and has been studied extensively over this foothill region. BC datasets (2009–2012) when examined showed that the BC concentrations in the foothills regions of the Himalayas were quite high as shown in Fig. 3.4, typical to that of the semi urban/urban site. BC levels were observed to show different diurnal variation (with two peaks; morning and evening peak with the daytime minimum BC) and seasonal variations with winter maximum at the site. This is in contrast to what was observed at the nearby site Nainital, where the diurnal variations result in a single afternoon peak in BC with maximum BC observed in the spring season. BC at the foothill site, was found to start increasing about an hour before sunrise, attaining the morning peak (linked with fumigation effect arising due to entrainment of BC aerosols from the nocturnal residual layer) within an hour or two and decreased afterwards during daytime. This resulted in lowest levels in the afternoon (due to turbulent mixing that dilutes the surface BC), followed by an increase after sunset attaining secondary peak in the evening, which then slowly decreases in the nighttime. The reduced mixing after sunset and rapid cooling of land leads to the formation of nocturnal layer resulting in the trapping of pollutants near surface during nighttime. The diurnal variations were clear and sharp in all the seasons at the foothill region showing maximum diurnal amplitudes in the winter season followed by autumn and minimum amplitude in summer-monsoon.

The impact of the local anthropogenic activities was also studied in terms of the weekly cycles in BC, which revealed a clear enhancement of $\sim 88\%$ in BC levels (in January) during weekdays, when compared with weekends levels. Higher BC in weekdays has been associated with traffic patterns and industrial activity (in nearby

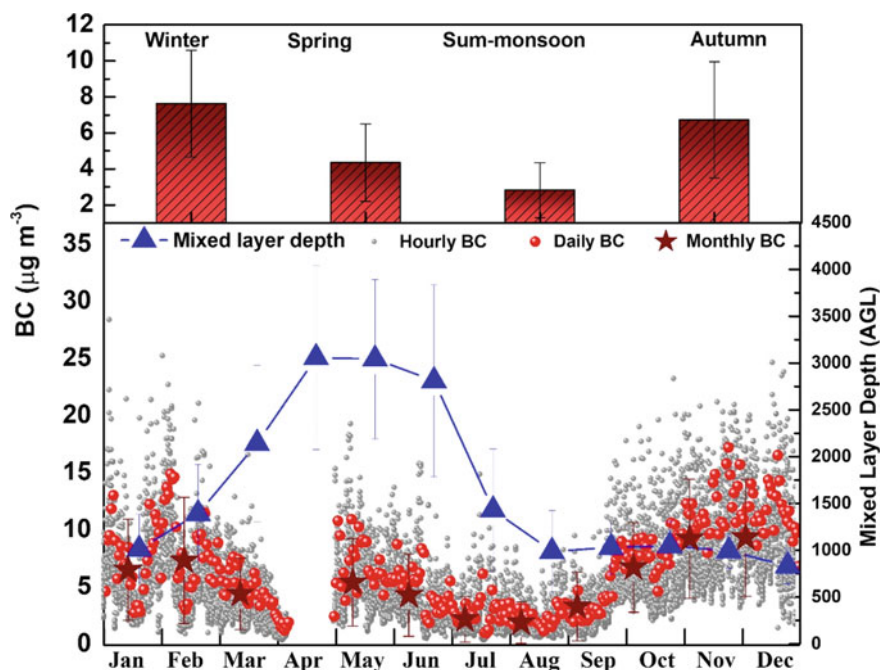


Fig. 3.4 Seasonal variations in BC mass concentrations (2009–2012), and seasonal mean noontime (1200–1400 h) mixing layer depth

region, within ~20 km) during weekdays, as compared to weekends with reduced industrial activity. The weekly variations in aerosols, however can be altered or completely masked by other factors like wind speed, wind direction, rainfall and long-range transport.

Investigation of the seasonal variation in BC when examined showed a maximum monthly mean BC in December ($9.3 \pm 5.1 \mu\text{g m}^{-3}$) and minimum in August ($1.9 \pm 1.8 \mu\text{g m}^{-3}$) (Fig. 3.4). BC was found to be maximum in winter ($7.9 \pm 5.2 \mu\text{g m}^{-3}$), the biomass/biofuel burning for cooking and heating purpose in winter was the possible major source of BC during this season. The minimum BC was reported in summer-monsoon ($2.8 \pm 2.8 \mu\text{g m}^{-3}$) (Fig. 3.4). The seasonal variation in BC shows reduction in the spring season at the foothill site. The reduction in the surface concentration of BC in spring season at the foothill region, despite the enhanced aerosol abundance in the spring season, was due to the extensive mixing of aerosols, as indicated by the mixing layer depth variation shown in Fig. 3.4. The aerosols near surface might have advected to the higher altitudes in spring. The observed BC concentration over the foothill site was then compared to what was observed at Nainital. BC was observed to be low at the Himalayan site (annual mean $\sim 1.0 \mu\text{g m}^{-3}$), while significant high BC ($\sim 5.50 \mu\text{g m}^{-3}$) was observed over the foothills site with different diurnal and seasonal variations. Seasonal mean BC was found to be maximum at the Himalayan site in spring, while at IGP, maximum BC was observed in winter. BC

was observed to be significantly high at foothills site in winter (~569%), followed by autumn (~543%), summer-monsoon (~304%) and spring (~240%) as compared to what observed at the Himalayan site. A clear evidence of the direct influence of aerosols from IGP to Himalayan region was observed in spring when the day to day variation in BC was in good association at these two sites. The possibility of direct transport was observed to be minimum in winter. The observed differences in BC, in particular in spring, provided the strong motivation to study the columnar abundance of the aerosols from the site and the spatial variation of aerosols over this region.

The columnar abundance of aerosols at the foothill site Pantnagar showed significant high AOD values with maximum columnar abundance of aerosol observed in the spring season (>0.6), which suggested that the surface level aerosols might have advected to the higher altitude regions in the spring leading to the low surface concentration of BC (along with other aerosols) while high total columnar abundance of aerosols. Monthly average AOD was maximum (>0.6) during late spring. The aerosol abundance was significant at the Pantnagar site throughout the year (annual mean AOD $\sim 0.56 \pm 0.32$). The significant aerosol abundance was observed in the foothills regions in the winter season (AOD > 0.4), suggesting a typical semi-urban/urban nature of the site. The observed different seasonal cycle of AOD, as compared to BC, at Pantnagar indicates the smaller contribution of BC in the total columnar abundance of aerosols by mass. The investigation of angstrom exponent revealed the presence of the coarse mode of aerosols during March–June at the site, as the site receives the significant amount of dust aerosols during this period. The columnar abundance of aerosol over the Himalayan site reveals very low AOD in fine mode (typical to clean free tropospheric site) in winter with significant aerosol load observed in spring dominated by coarse mode of aerosols. The spatial variation of AOD from MODIS and absorbing aerosols (retrieved aerosol index) from the Ozone Monitoring Instrument (OMI) also showed maximum loading in the spring season.

3.5 Role of Mixing Layer Depth and BC-CO Relation

The influence and variations in planetary boundary layer height on the surface evolution of BC was explored by investigating the association between BC and mixing layer depth (MLD). The MLD plays an important role in determining the concentration of pollutants near surface and their distribution above the surface. It represents the volume available for dispersion of pollutants due to convection or mechanical turbulence. Due to lack of the ground-based observations of the planetary boundary layer height at the site, the MLD height was calculated using HYSPLIT model. The influence of the MLD in BC was examined at the low altitude foothills site, which also helped in understanding the uplifting of aerosols to the nearby higher altitude regions. The noon-time (1200–1400 h, IST) MLD estimation was carried out around Pantnagar ($1^\circ \times 1^\circ$), which showed MLD to be maximum in April–June (higher solar radiation and surface temperature), which then decreased to about 1000 m during August–January with a minimum value of $\sim 832 \pm 193$ m in December as shown in

Fig. 3.4. The reduction in the solar radiation, cloudy conditional and rainfall causes reduction in MLD during monsoon. Interestingly, the higher BC level in winter ($7.9 \pm 5.2 \mu\text{g m}^{-3}$) and autumn ($6.5 \pm 4.9 \mu\text{g m}^{-3}$) was found to coincide with lower values of MLD during these seasons (about 1050 m) indicating that the mixing of BC emitted from sources is limited to quite a less volume as compared to spring and summer seasons (Fig. 3.5).

In order to better understand the evolution of BC with MLD, the daytime (1100–1700 h) variation in BC and MLD was studied and is shown in Fig. 3.5. Interestingly, an inverse association, with highest anti-correlation ($R^2 = 0.89$) is observed in winter followed by autumn ($R^2 = 0.76$) and spring ($R^2 = 0.61$) was found while minimum association was found in monsoon (July–August) ($R^2 = 0.33$). It was found that the variations in MLD had a strong role in governing wintertime BC, while MLD played a weak role during the monsoon period when the observation site is under the influence of the rainfall, and receives intense air-masses from oceanic regions.

The variation in BC and Carbon monoxide (CO) was then explored, both of which were found to be governed by similar evolution with MLD. The common sources of combustion were identified by utilizing the BC-CO relation for the first time over the Indian region. Both BC and CO have been linked closely with each other via combustion process, as the type and amount of combustion changes their emission ratio in the combustion process (Seinfeld and Pandis 1998). The CO observations were made using non-dispersive infrared ($4.6 \mu\text{m}$) absorption technique. The useful information regarding the influence of fresh and aged air masses at the site was accessed by utilizing the BC-CO association. A strong correlation indicates common combustion source with influence of fresh emission, while poor correlation indicates emission from diverse sources and aged emissions. BC and CO reveals a good correlation in winter ($R^2 = 0.75$) and late autumn seasons ($R^2 = 0.72$) indicating the presence of similar types of combustion sources (Fig. 3.5c). The positive correlation ($R^2 = 0.62$) was observed in spring, however a poor correlation ($R^2 = 0.05$) was observed in summer-monsoon. The marine air masses arrive from diverse directions in summer-monsoon, which cause scavenging of aerosols and gases over the region, but these air masses sometimes carry aerosols (from diverse regions) along with them to the site, which leads to the observed poor correlation between BC and CO during this season. In addition, due to different lifetime of BC and CO (CO possesses much longer lifetime than BC), and due to different processes of scavenging BC than CO showed poor correlation. The dominant BC emissions were then indicated from the average slope of BC-CO (BC versus CO) over this region. The observed slope was found to be $\sim 10.4 \mu\text{g ppmv}^{-1}$, which was even higher than what was observed over Mexico and Germany (Baumgardner et al. 2002). The influence from cooking/domestic use of fuel was indicated as the main contributor.

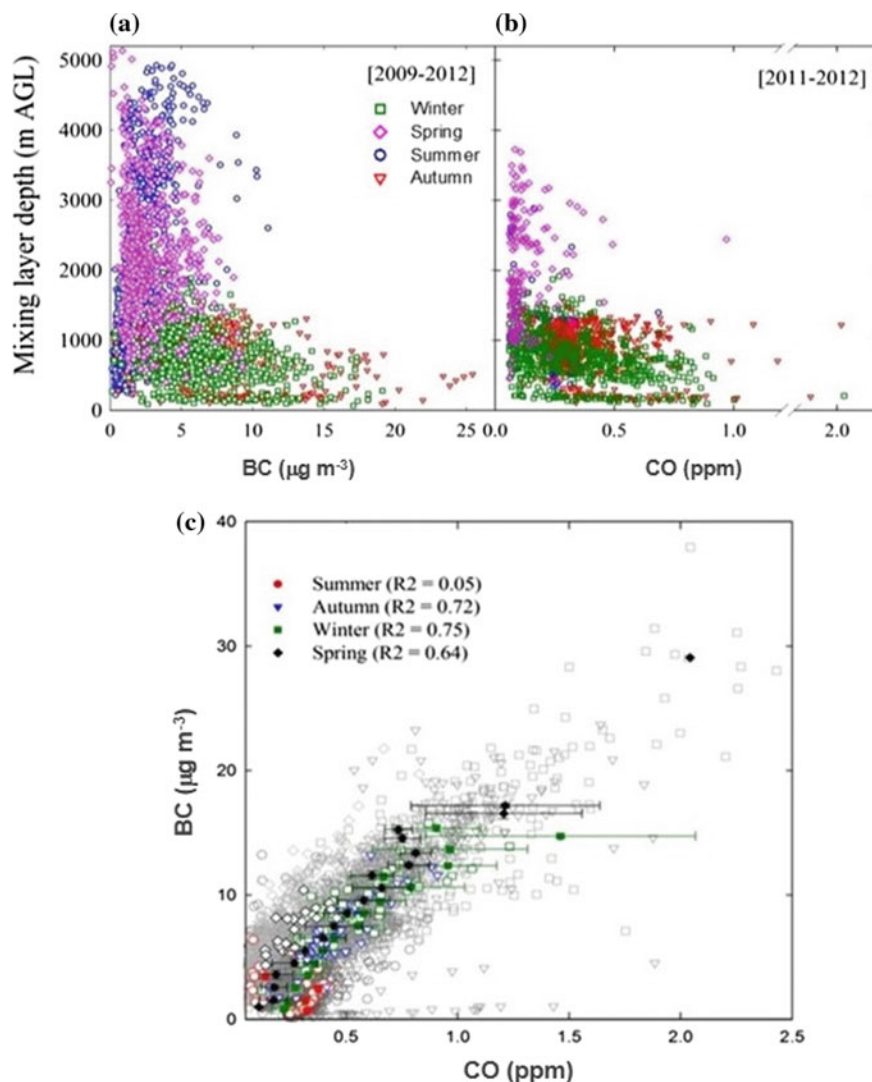


Fig. 3.5 **a, b** Correlation of hourly daytime (1100–1700 h) BC ($\mu\text{g m}^{-3}$) and carbon monoxide (CO) with mixed layer depth (m AGL) for different seasons at Pantnagar. **c** The hourly average correlation between surface CO and BC is shown by open grey symbols. The daily average (color open symbols) and binned averages (color filled symbols) correlation between CO and BC is also shown

3.6 Association of BC with Large-Scale Wind Patterns: Source Distributions

The influence of large-scale winds in the observed BC mass concentration was studied at the foothill site. The seven-days back-air trajectories were calculated utilizing the Hybrid Single-Particle Lagrangian Integrated Trajectory (HYSPPLIT; Draxler and Rolph 2003) model and using the NCEP/NCAR global reanalysis data at 1000 m AGL at Pantnagar. The trajectories were calculated and clustered according to the ward's Hierarchical method by combining the nearest trajectories according to angular distance in order to determine the direction of arrival of air masses to the site. The calculated trajectories were then clustered as shown in Fig. 3.6. The trajectories in different seasons were then clustered in five different groups west (W), north-west (NW), north-east (NE), south-west (SW) and south-east (SE), based on the direction from which they were originating (Fig. 3.6). It was found that the site was influenced by the air masses originating from W and NW with a larger contribution from the NW group (~63%) in winter and from W group (55%) in spring. The marine air

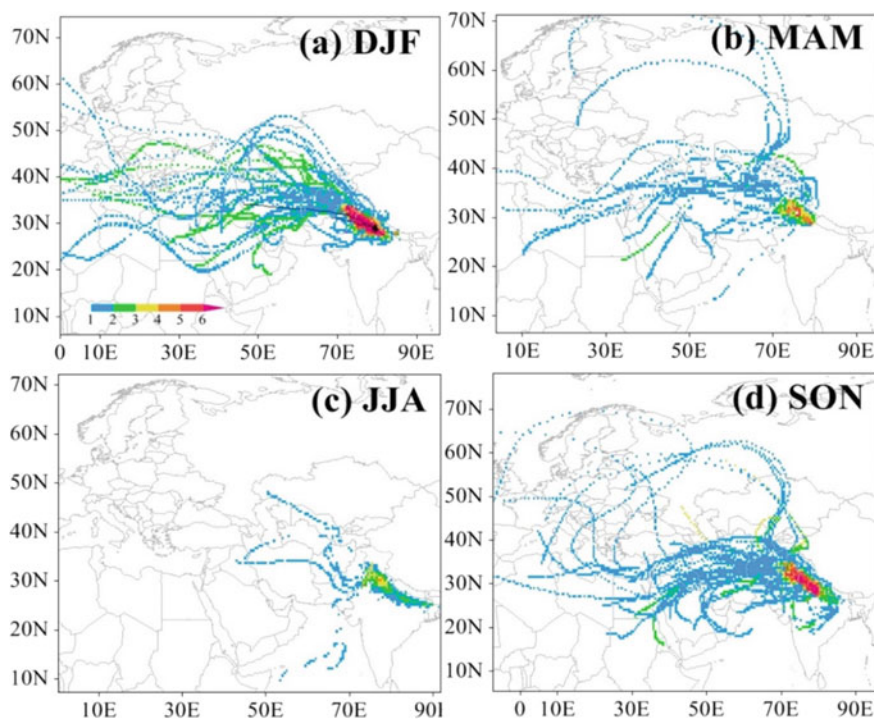


Fig. 3.6 Seasonal source apportionment using BC concentrated weighted trajectories during different seasons, winter (December–February), spring (March–May), summer-monsoon (June–August) and autumn (September–November) of 2009–2012. The color bar represents the BC mass concentration in $\mu\text{g m}^{-3}$

masses contribute ~63% (both SW and SE) from the oceanic regions of the Bay of Bengal (SE) and the Arabian Sea (SW), while ~37% of air masses of continental origin from NW directions. The change in the air mass pattern was again observed in autumn. The dominance of air masses originating from continental origin from W/NW was observed, while air masses arriving from marine origin from SE were reduced due to the withdrawal of the southwest monsoon from the Indian region.

The possible source regions contributing to the observed BC at the foothill site was investigated by the means of Concentration Weighted Trajectory (CWT) analysis (Stohl 1996). In this method, a grid was superimposed over the domain of all the trajectories computed and the weighted value of observed concentration was assigned to the trajectories that crossed the corresponding grid cell. The study revealed maximum BC contribution from NW and W ~ 7–8 $\mu\text{g m}^{-3}$ in both winter and autumn. In winter, air masses arriving from the NW direction (~62% of air masses) contribute significant BC of ~8.54 $\mu\text{g m}^{-3}$. The change in the air masses was observed in the spring season when air masses shift from NW (45%) to W (55%). The air-masses from the W sector contributes BC of ~4.89 $\mu\text{g m}^{-3}$. In summer-monsoon, influence of SE (38%) and SW (24%) air masses were seen, with BC levels dropping to 2.21–2.59 $\mu\text{g m}^{-3}$. Soon after the withdrawal of the southwest monsoon, the dominant contribution from NW direction was again seen in autumn, with a consequent rise in BC levels (7.89 $\mu\text{g m}^{-3}$). The air masses that passed through the IGP region with higher amount of BC, before arriving at the foothill site have been reported to contribute to the observed BC at the site. The observed levels at the foothill site were found to be influenced and augmented by the synoptic air masses arriving via IGP, especially due north-west (NW) of the site.

3.7 Simulations of BC Using WRF-Chem

The observations of BC at the foothills site were used to assess the ability of WRF-Chem model in simulating seasonal and diurnal variability in BC. The model domain was kept centered at Pantnagar (79.5° E, 29.0° N) with (100, 100, 37) grid points in (x longitude, y latitude, z vertical) directions with horizontal grid spacing of 10 km and the model top located at 50 hPa. The model simulations were made for January, May and July (due to computational limitation) representing winter, spring and summer/monsoon seasons. The comparison of temporal variation in BC showed high temporal variation in the observed BC, while the model was able to capture some of temporal variation, but the magnitude was highly underestimated by the model (Fig. 3.7).

It was quite interesting that the model simulated BC at 29 N (representing the site by model simulations) was quite low with low episodic enhancements, while BC simulations at 28 N (representing the IGP regions far away from foothill region) was higher in magnitude. These simulations indicated the presence of large spatial variability in BC emissions around the foothill site especially in winter. Further, the day to day variability in BC was highly underestimated by the model. The model

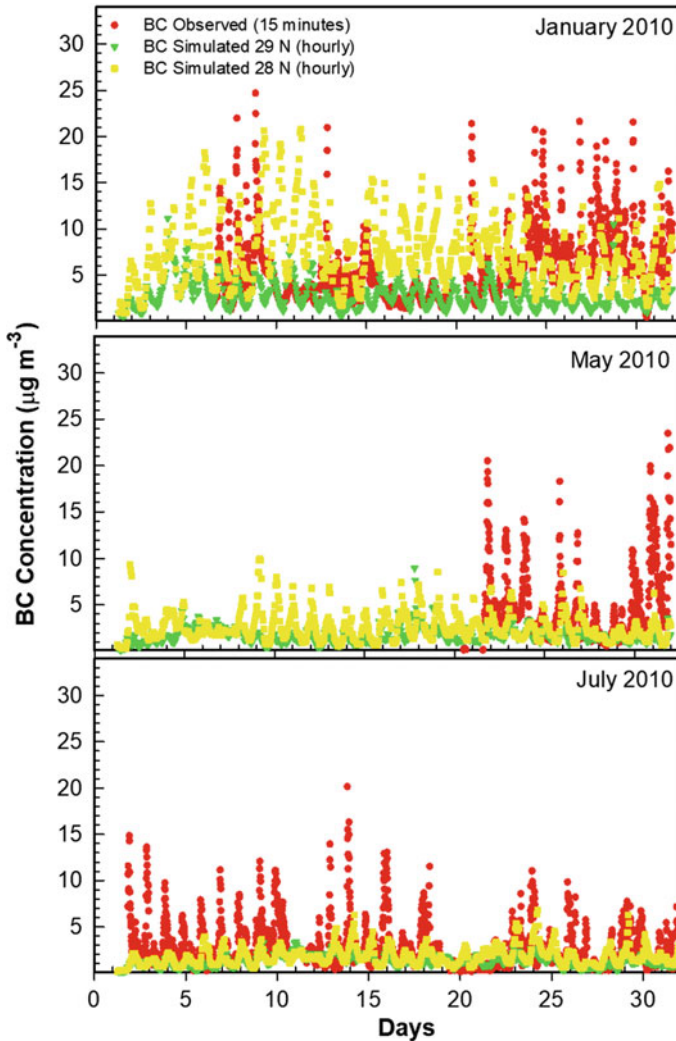


Fig. 3.7 The comparison of temporal variation in observed BC mass concentration with model simulated BC at Pantnagar for year 2010

performance in simulating the diurnal variability in BC was also investigated as the studies on diurnal pattern simulations of BC over the Indian region were sparse.

The model showed a mixed capability in simulating BC diurnal variation as shown in Fig. 3.8. The model was found to capture some features, while missed out on a few others. The high observed BC during nighttime and low BC during daytime as a result of diurnal changes in the planetary boundary layer height was captured by the model. The morning and evening peaks in observed BC were not captured by the model possibly due to the inadequacy of the ABL schemes in the model (as has been

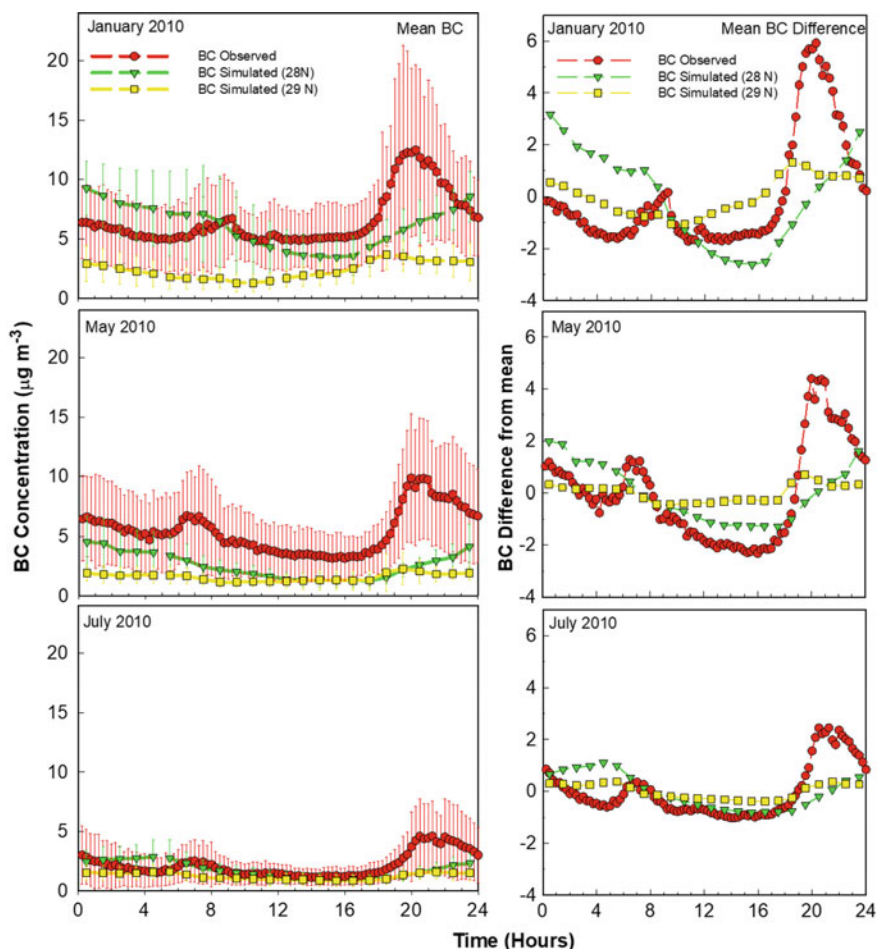


Fig. 3.8 Diurnal variations in observed BC and WRF-Chem model simulated BC during January, May and July (left panel) for year 2010. The difference in the diurnal variation in BC for observed and simulated BC from their respective mean BC (right panel)

pointed out by some earlier reports; (Nair et al. 2012; Moorthy et al. 2013b) using RegCM and GOCART models). Average observed and modeled BC at Pantnagar during January, May and July were 6.6 ± 2.2 and $2.4 \pm 1.2 \mu\text{g m}^{-3}$, 5.5 ± 1.8 and $1.6 \pm 0.7 \mu\text{g m}^{-3}$, and 2.2 ± 1.0 and $1.2 \pm 0.5 \mu\text{g m}^{-3}$, respectively. The BC levels simulated at 28 N were found to be $6.1 \pm 3.1 \mu\text{g m}^{-3}$, $2.5 \pm 1.6 \mu\text{g m}^{-3}$ and $1.8 \pm 1.0 \mu\text{g m}^{-3}$ for January, May and July, respectively. These average levels at 28 N were found to be in a good agreement with observations.

The model was able to capture the observed decrease in BC from January to July indicating the capability of the model to qualitatively capture the seasonal variations

in BC. The model however failed to capture BC levels, thus the decrease in the magnitude of seasonal and diurnal variation in BC was underestimated. Additionally, the role of meteorology in controlling seasonal and diurnal variation in BC at Pantnagar was also highlighted as BC emissions provided as input to the model do not have a seasonal cycle. The WRF-Chem model was found to capture some of the observed features but in order to capture the observed magnitude in good agreement, improvement in the diurnal and seasonal variability in the BC emission sources in and around the foothills region was strongly suggested. In addition, need of co-located observations of planetary boundary layer height were suggested for better evaluation of model performance over the region.

3.8 Vertical Distribution of Aerosols Over the Region

In order to understand the aerosols variation at the foothill location and its vertical distribution above the site, aerosol vertical profiles from CALIPSO were examined. The aerosol profiles in different seasons were examined, which showed the confinement of aerosol over the low altitude regions in winter and autumn, while significant presence of aerosols to greater vertical extension (~about 4–5 km altitude) in spring and early summer (Fig. 3.9). The seasonal variation in aerosols was then explored in detail for which the aerosol extinction profiles were investigated at the foothill site. The cloud free and quality controlled CALIPSO extinction profiles (532 nm) were examined at 2×2 degree around Pantnagar.

The daytime and nighttime profiles of aerosols extinction coefficient were examined for days when the surface BC showed enhancement. The higher extinction coefficient near ground was observed in the nighttime profiles, which sharply decreased above ~1 km as compared to the daytime profile (Fig. 3.10). The surface BC, although constituting a minor fraction of columnar AOD, was reported to significantly affect the aerosol properties, especially in winter when most of the aerosols (including BC) are strongly confined near surface usually below ~1 km. The daytime levels in BC, mixing layer depth and daytime profile of extinction coefficient at the Pantnagar site when showed the possibility of uplifting and mixing of aerosols (including BC) to higher heights.

The seasonal variation in aerosols extinction coefficient at 532 nm as shown in Fig. 3.10 revealed high aerosol extinction coefficient (more than 2 km^{-1}) near surface in winter, which decreased sharply to less than 0.25 km^{-1} at about 1.5 km indicating the strong confinement of aerosols below 2 km. The vertical profile of aerosols extinction coefficient showed similar variation as that in winter but the aerosol extinction coefficient value near surface are found to be low as compared to the winter when quite high extinction coefficient was observed near surface. The vertical gradient in the aerosol extinction coefficient was also smaller in spring indicating mixing of aerosols between surface and ~3 km. Aerosol profiles in spring season also revealed reduction in the aerosol extinction coefficient near surface, while enhancement at the higher altitude regions.

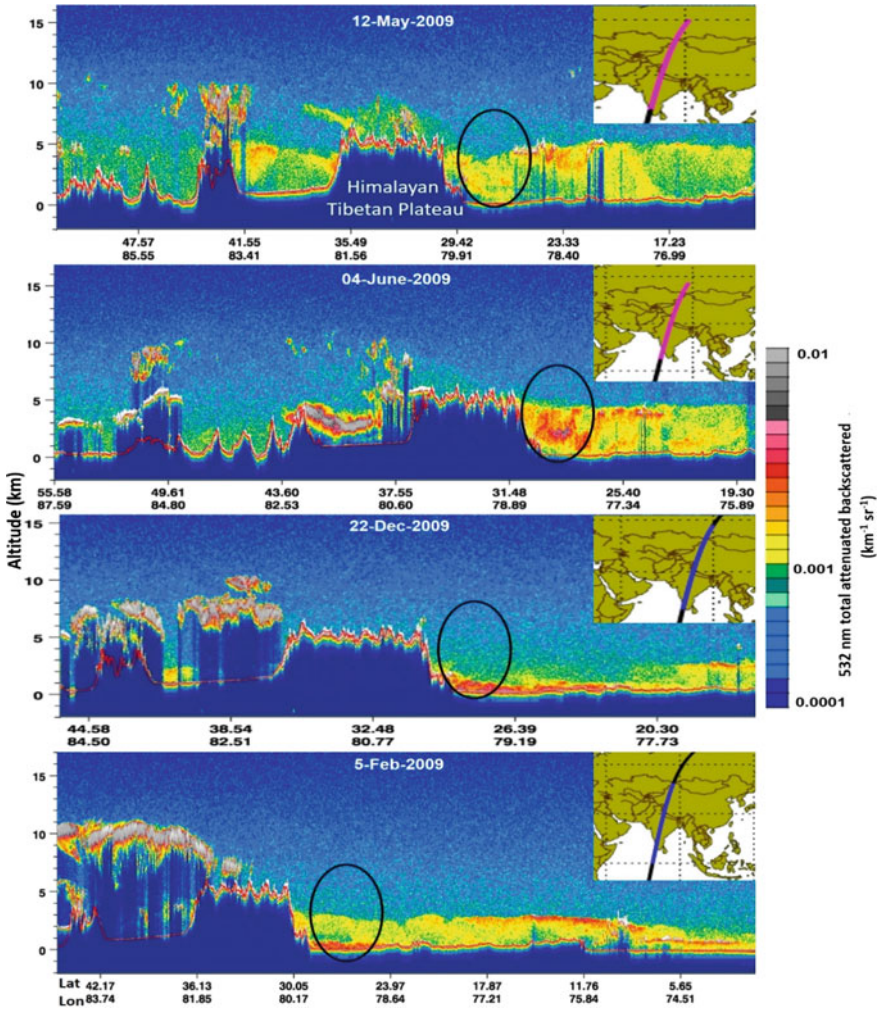


Fig. 3.9 CALIPSO, 532 nm total attenuated backscattered profiles ($\text{km}^{-1} \text{sr}^{-1}$) from southern India to the Himalayan Tibetan Plateau region (HTP). The orbital track of each profile is also shown. The profiles were investigated for 12 May 2009, representing spring, 4 June 2009 representing early summer, and 22 Dec 2009 and 5 Feb 2009 representing winter season

3.9 Conclusions

The variability of aerosols over the high-altitude region in the central Himalayas and its adjacent foothills location was studied. The sources and the processes governing the distribution of aerosols at these sites was explored. The decadal scale ground-based aerosol observations were used to present the climatology and trends of aerosols at the high altitude, regional representative site in the central Himalayas. The

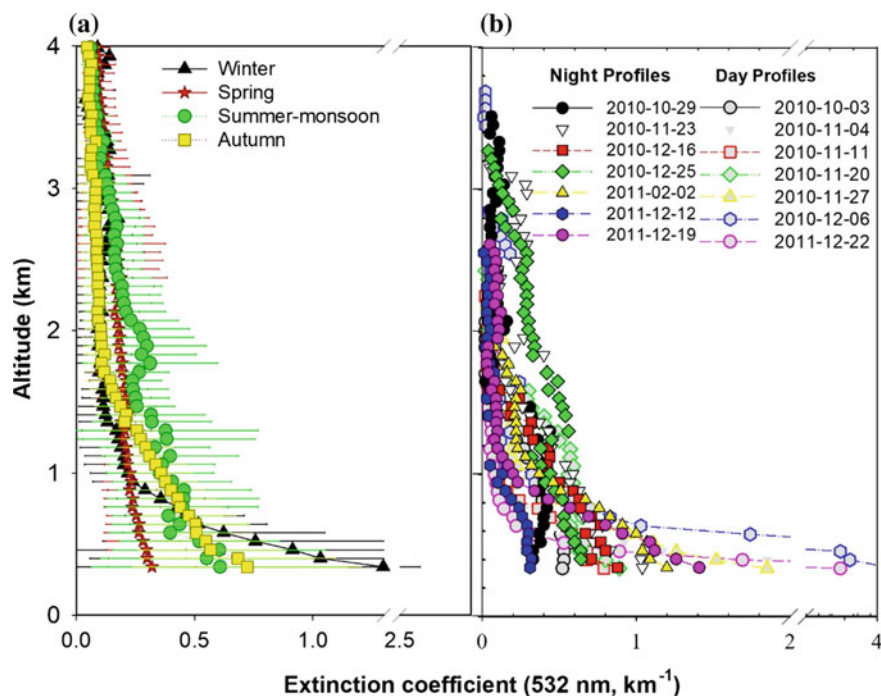


Fig. 3.10 **a** Seasonal profiles of aerosol extinction coefficients at 532 nm from CALIPSO during 2010–2011 for different seasons. **b** Variation in the aerosol extinction coefficient corresponding to high BC days

enhancement in the black carbon aerosols and columnar abundance in the aerosols was observed at the site. The observed positive trend in black carbon (BC) was found to be $\sim 1.511 \text{ ng m}^{-3}$ per year with a standard error (σ_{ω}) of ~ 0.975 , indicating increase in the absorbing aerosols over this region. The columnar abundance of aerosols (AOD at 500 nm) also showed an increasing trend of ~ 0.000774 per year with a standard error (σ_{ω}) of ~ 0.000415 . The increasing trends in aerosol abundance and BC indicate the more warming potential of aerosol over this region. The regional characterization of aerosols was made from the adjacent foothill site in the Indo-Gangetic Plain region in order to understand the sources of aerosols, and aerosol characterization near the source region. The influence of aerosol sources from the IGP region to the nearby Himalayan region were studied. The foothill region was found to be marked with high levels of BC mass concentration as well as the columnar loading of aerosols. Large variations were observed in BC at diurnal and seasonal scales, closely associated with the local/regional anthropogenic influences, mesoscale and synoptic meteorological processes.

The influence of the local emissions and the atmospheric boundary layer dynamics was examined in the diurnal variations in BC. The mixing layer depth was observed to play a dominant role in governing the surface distribution of BC in winter. BC

exhibited nearly an inverse relation with MLD in all seasons, which was found to be strongest in winter and weakest in monsoon. The influence of fresh emissions with common combustion sources were observed in winter and autumn, while the influence of aged air mass and emissions from different combustion sources were witnessed in summer-monsoon.

Unlike BC, the co-located study of aerosol optical depths (AOD) and aerosol absorption reveals maximum in spring over IGP, possibly due to the presence of absorbing aerosols (including BC, dust) above the ABL (in the free troposphere). The aerosol optical depth (AOD 500 nm) variation shows annual peak in May–June. The dominance of coarse mode of aerosols was found in spring and early summer, while dominance of fine mode of aerosols was found in late autumn and early winter.

The influence of the large-scale winds was also studied at the foothill site, which revealed that the air masses arriving through the IGP region contribute to the BC observed at the site. The vertical profile of aerosol from CALIPSO satellite showed sharp confinement of aerosols near surface in winter followed by autumn in the IGP region, while aerosols were observed to reach the high-altitude Himalayan regions in spring season. The aerosol extinction coefficient values were found to be quite high near surface in winter over the IGP region. In spring, the reduction in aerosol extinction coefficient was observed near surface (over IGP region) while it showed enhancement in the higher altitudes (altitudes >2 km).

The performance of the WRF-Chem model was also evaluated in simulating the observed ground based black carbon aerosols over the foothill regions in IGP. The improvement in the emission inventory with finer temporal and spatial resolution in the IGP region, along with the boundary layer measurements was strongly suggested in order to capture and match the actual levels of aerosols observed over this region by the present-day models, which can then be used for accurate impact assessment of aerosols over this region.

Acknowledgements The present work was carried out under ISRO-GBP (ARFI) project. The authors highly acknowledge the ISRO-GBP (ARFI) and ISRO-GBP (ATCTM) projects. The author HJ wants to acknowledge Dr. Rajesh Kumar for providing the WRF model simulations. The CO data was obtained from Piyush Bhardwaj. The help and support received from Prof. K. P. Singh during measurement at Pantnagar site is highly acknowledged. Special thanks to the PI of AERONET site at Pantnagar for providing quality assured data. The satellite datasets of aerosols were obtained from MODIS via Giovanni site, and CALIPSO from NASA Langley Research Center Atmospheric Science Data Center. The HYSPLIT model made available from NOAA Air Resources Laboratory was also used and is acknowledged.

References

- Agnihotri R, Mandal TK, Karapurkar SG, Naja M, Gadi R, Ahammmed YN, Kumar A, Saud T, Saxena M (2011) Stable carbon and nitrogen isotopic composition of bulk aerosols over India and northern Indian Ocean. *Atmos Environ* 45:2828–2835. <https://doi.org/10.1016/j.atmosenv.2011.03.003>
- Alfaro SC, Gaudichet A, Gomes L, Maillé M (1997) Modeling the size distribution of a soil aerosol produced by sandblasting. *J Geophys Res* 102(D10):11239–11249. <https://doi.org/10.1029/97JD00403>
- Angstrom, A. (1964) The parameters of atmospheric turbidity. *Tellus* 16(1):64–75
- Babu SS, Manoj M, Moorthy KK, Gogoi M, Nair V, Kompalli S, Satheesh SK, Niranjan K, Ramagopal K, Bhuyan PK, Singh D (2013) Trends in aerosol optical depth over Indian region: potential causes and impact indicators. *J Geophys Res: Atmos* 118:11794–11806
- Baumgardner D, Raga GB, Peralta O, Rosas I, Castro T, Kuhlbusch T, John A, Petzold A (2002) Diagnosing black carbon trends in large urban areas using carbon monoxide measurements. *J Geophys Res: Atmos* 107(D21):8342. <https://doi.org/10.1029/2001jd000626>
- Blanchard DC (1985) The oceanic production of atmospheric sea salt. *J Geophys Res* 90:961–963
- Bodhaine BA (1995) Aerosol absorption measurements at Barrow, Mauna Loa and the south pole. *J Geophys Res* 100(D5):8967–8975. <https://doi.org/10.1029/95JD00513>
- Bonasoni P, Laj P, Marinoni A, Sprenger M, Angelini F, Arduini J, Bonafe U, Calzolari F, Colombo T, Decesari S, Di Biagio C, di Sarra AG, Evangelisti F, Duchi R, Facchini MC, Fuzzi S, Gobbi GP, Maione M, Panday A, Roccatò F, Sellegri K, Venzac H, Verza GP, Villani P, Vuillermoz E, Cristofanelli P (2010) Atmospheric Brown Clouds in the Himalayas: first two years of continuous observations at the Nepal-Climate Observatory at Pyramid (5079 m). *Atmos Chem Phys Discuss* 10:4823–4885
- Bond TC, Doherty SJ, Fahey DW, Forster PM, Berntsen T, DeAngelo BJ, Flanner MG, Ghan S, Kärcher B, Koch D, Kinne S, Kondo Y, Quinn PK, Sarofim MC, Schultz MG, Schulz M, Venkataraman C, Zhang H, Zhang S, Bellouin N, Guttikunda SK, Hopke PK, Jacobson MZ, Kaiser JW, Klimont Z, Lohmann U, Schwarz JP, Shindell D, Storelvmo T, Warren SG, Zender CS (2013) Bounding the role of black carbon in the climate system: a scientific assessment. *J Geophys Res Atmos* 118:5380–5552. <https://doi.org/10.1002/jgrd.50171>
- Boucher O, Randall D, Artaxo P, Bretherton C, Feingold, G, Forster P, Kerminen V-M, Kondo Y, Liao H, Lohmann U, Rasch P, Satheesh SK, Sherwood S, Stevens B, Zhang XY (2013) Clouds and aerosols. In: *Climate change 2013: the physical science basis. Contribution of Working Group I to the fifth assessment report of the Intergovernmental Panel on Climate Change*. Cambridge University Press, USA
- Charlson RJ, Langner J, Rodhe H, Leovy CB, Warren SG (1991) Perturbation of the northern hemisphere radiative balance by backscattering from anthropogenic sulfate aerosols. *Tellus* 43A:152–163
- Charlson RJ, Schwartz SE, Hales JM, Cess RD, Coakley JA, Hansen JE, Hofmann DJ (1992) Climate forcing by anthropogenic aerosols. *Science* 255:423–430
- Chin M, Ginoux P, Kinne S, Torres O, Holben BN, Duncan BN, Martin RV, Logan JA, Higurashi A, Nakajima T (2002) Tropospheric aerosol optical thickness from the GOCART model and comparisons with satellite and sunphotometer measurements. *J Atmos Sci* 59:461–483
- Dey S, Tripathi SN, Singh RP (2004) Influence of dust storms on the aerosol optical properties over the Indo-Gangetic basin. *J Geophys Res* 109:D20211. <https://doi.org/10.1029/2004JD004924>
- Draxler RR, Rolph GD (2003) Real-time environmental applications and display system (READY). NOAA Air Resources Laboratory, Silver Spring, MD. <http://www.arl.noaa.gov/ready/hysplit4.html>
- Dumka UC, Moorthy KK, Pant P, Hegde P, Sagar R, Pandey K (2008) Physical and optical characteristics of atmospheric aerosols during ICARB at Manora Peak, Nainital: a sparsely inhabited, high-altitude location in the Himalayas. *J Earth Syst Sci* 117(S1):399–405

- Dumka UC, Moorthy KK, Kumar R, Hegde P, Sagar R, Pant P, Singh N, Babu SS (2010) Characteristics of aerosol black carbon mass concentration over a high altitude location in the Central Himalayas from multi-year measurements. *Atmos Res* 96:510–521. <https://doi.org/10.1016/j.atmosres.2009.12.010>
- Eck TF, Holben BN, Reid JS, Dubovik O, Kinne S, Smirnov A, O'Neill NT, Slutsker I (1999) The wavelength dependence of the optical depth of biomass burning, urban and desert dust aerosols. *J Geophys Res* 104:31333–31350
- Fitzgerald JW (1991) Marine aerosols: a review. *Atmos Environ* 25A:533–545
- Flanner MG, Zender CS, Hess PG, Mahowald NM, Painter TH, Ramanathan V, Rasch PJ (2009) Springtime warming and reduced snow cover from carbonaceous particles. *Atmos Chem Phys* 9(7):2481–2497. <https://doi.org/10.5194/acp-9-2481-2009>
- Gautam R, Hsu NC, Tsay S-C, Lau WK, Holben B, Bell S, Smirnov A, Li C, Hansell R, Ji Q, Payra S, Aryal D, Kayastha R, Kim KM (2011) Accumulation of aerosols over the Indo-Gangetic plains and southern slopes of the Himalayas: distribution, properties and radiative effects during the 2009 pre-monsoon season. *Atmos Chem Phys* 11:12841–12863. <https://doi.org/10.5194/acp-11-12841-2011>
- Gautam R, Hsu NC, Lau K-M (2010) Premonsoon aerosol characterization and radiative effects over the Indo-Gangetic Plains: implications for regional climate warming. *J Geophys Res* 115:D17208. <https://doi.org/10.1029/2010JD013819>
- Giles DM, Holben BN, Tripathi SN, Eck TF, Newcomb WW, Slutsker I, Dickerson RR, Thompson AM, Mattoo S, Wang S-H, Singh RP, Sinyuk A, Schafer JS (2011) Aerosol properties over the Indo-Gangetic Plain: a mesoscale perspective from the TIGERZ experiment. *J Geophys Res* 116:D18203. <https://doi.org/10.1029/2011JD015809>
- Gobbi GP, Angelini F, Bonasoni P, Verza GP, Marinoni A, Barnaba F (2010) Sunphotometry of the 2006–2007 aerosol optical/radiative properties at the Himalayan Nepal Climate Observatory—Pyramid (5079 m a.s.l.). *Atmos Chem Phys Discuss* 10:1193–1220
- Grell GA et al (2005) Fully coupled “online” chemistry within the WRF model. *Atmos Environ* 39:6957–6975
- Hansen AD, Rosen AH, Novakov T (1984) The Aethalometer—an instrument for the real-time measurement of optical absorption by aerosol particles. *Sci Total Environ* 36:191–196. [https://doi.org/10.1016/0048-9697\(84\)90265-1](https://doi.org/10.1016/0048-9697(84)90265-1)
- Hansen JE, Sato M, Lacis A, Ruedy R, Tegen I, Matthews E (1998). Climate forcings in the industrial era. *Proc Natl Acad Sci* 12753–12758
- Haywood JM, Ramaswamy V (1998) Global sensitivity studies of the direct radiative forcing due to anthropogenic sulfate and black carbon aerosols. *J Geophys Res* 103:6043–6058
- Hegde P, Pant P, Naja M, Dumka UC, Sagar R (2007). South Asian dust episode in June 2006: aerosol observations in the Central Himalayas. *Geophys Res Lett* 34:L23802. <https://doi.org/10.1029/2007gl030692>
- Hinds W (1999) *Aerosol technology: properties, behavior, and measurement of airborne particles*. Wiley, New York
- Holben BN, Tanre D, Smirnov A, Eck TF, Slutsker I, Abuhassan N, Newcomb WW, Schafer JS, Chatenet B, Lavenu F, Kaufman YJ, Vande Castle J, Setzer A, Markham B, Clark D, Frouin R, Halthore R, Karneli A, O'Neill NT, Pietras C, Pinker RT, Voss K, Zibordi G (2001) An emerging ground-based aerosol climatology: aerosol optical depth from AERONET. *J Geophys Res* 106(D11):12067–12097
- Holben BN, Eck TF, Slutsker I, Tanré D, Buis JP, Setzer A, Vermote E, Reagan JA, Kaufman YJ, Nakajima T, Lavenu F, Jankowiak I, Smirnov A (1998) AERONET—a federated instrument network and data archive for aerosol characterization. *Remote Sens Environ* 66:1–16
- Ichoku C, Levy L, Kaufman YJ, Remer LA, Rong-Rong L, Martins VJ, Holben BN, Abuhassan N, Slutsker I, Eck TF, Pietras C (2002) Analysis of the performance characteristics of the five-channel Microtops II sun photometer for measuring aerosol optical thickness and precipitable water. *J Geophys Res* 107:D13. <https://doi.org/10.1029/2001JD001302>

- IPCC (2007) Summary for policymakers. In: Solomon S, Qin D, Manning M, Chen Z, Marquis M, Averyt KB, Tignor M, Miller HL (eds) *Climate change 2007: the physical science basis. Contribution of Working Group I to the fourth assessment report of the Intergovernmental Panel on Climate Change*. Cambridge University Press, Cambridge, United Kingdom/New York, NY, USA
- Jacobson MZ (2001) Strong radiative heating due to the mixing state of black carbon in atmospheric aerosols. *Nature* 409:695–697
- Jain SK (2008) Impact of retreat of Gangotri glacier on the flow of Ganga River. *Curr Sci* 95:1012–1014
- Janssens-Maenhout G et al (2012) EDGAR-HTAP: a harmonized gridded air pollution emission dataset based on national inventories. EUR Report No. EUR 25229, European Commission Publications Office, Ispra, Italy, p 40
- Joshi H, Naja M, Singh KP, Kumar R, Bhardwaj P, Babu SS, Sathesh SK, Moorthy KK, Chandola HC (2016) Investigations of aerosol black carbon from a semi-urban site in the Indo-Gangetic Plain region. *Atmos Environ*. <https://doi.org/10.1016/j.atmosenv.2015.04.007>
- Junge CE (1963) *Air chemistry and radioactivity*. Academic Press, New York
- Koch D, Hansen J (2005) Distant origins of Arctic black carbon: a Goddard Institute for Space Studies ModelE experiment. *J Geophys Res* 110:D04204. <https://doi.org/10.1029/2004JD005296>
- Kulkarni AV, Bahuguna IM, Rathore BP, Singh SK, Randhawa SS, Sood RK, Dhar S (2007) Glacial retreat in Himalaya using Indian Remote Sensing Satellite data. *Curr Sci* 92(1):69–74
- Kumar R, Naja M, Sathesh SK, Ojha N, Joshi H, Sarangi T, Pant P, Dumka UC, Hegde P, Venkataramani S (2011) Influences of the springtime northern Indian biomass burning over the central Himalayas. *J Geophys Res* 116:D19302. <https://doi.org/10.1029/2010JD015509>
- Kumar R, Naja M, Pfister GG, Barth MG, Brasseur GP (2012) Simulations over South Asia using the Weather Research and Forecasting model with Chemistry (WRF-Chem): set-up and meteorological evaluation. *Geosci Model Dev* 5:321–343. <https://doi.org/10.5194/gmd-5-321-2012>
- Lau K-M, Kim K-M (2006) Observational relationships between aerosol and Asian monsoon rainfall, and circulation. *Geophys Res Lett* 33:L21810. <https://doi.org/10.1029/2006GL027546>
- Lau KM, Kim M, Kim K, Lee W (2010) Enhanced surface warming and accelerated snow melt in the Himalayas and Tibetan Plateau induced by absorbing aerosols. *Environ Res Lett* 5:025204. <https://doi.org/10.1088/1748-9326/5/2/025204>
- Lawrence MG, Lelieveld J (2010) Atmospheric pollutant outflow from southern Asia: a review. *Atmos Chem Phys* 10:11017–11096. <https://doi.org/10.5194/acp-10-11017-2010>
- Lelieveld J, Crutzen PJ, Ramanathan V, Andreae MO, Brenninkmeijer CAM, Campos T, Cass GR, Dickerson RR, Fischer H, de Gouw JA, Hansel A, Jefferson A, Kley D, de Laat ATJ, Lal S, Lawrence MG, Lobert JM, Mayol-Bracero OL, Mitra AP, Novakov T, Oltmans SJ, Prather KA, Reiner T, Rodhe H, Scheeren HA, Sikka D, Williams J (2001) The Indian Ocean experiment: widespread air pollution from South and Southeast Asia. *Science* 291(5506):1031–1036. <https://doi.org/10.1126/science.1057103>
- Lu Z, Streets DG, Zhang Q, Wang S (2012) A novel back-trajectory analysis of the origin of black carbon transported to the Himalayas and Tibetan Plateau during 1996–2010. *Geophys Res Lett* 39:L01809. <https://doi.org/10.1029/2011GL049903>
- Marinoni A, Cristofanelli P, Laj P, Duchì R, Calzolari F, Decesari S, Sellegri K, Vuillermoz E, Verza GP, Villani P, Bonasoni P (2010) Aerosol mass and black carbon concentrations, a two year record at NCO-P (5079 m, Southern Himalayas). *Atmos Chem Phys* 10:8551–8562. <https://doi.org/10.5194/acp-10-8551-2010>
- Menon S, Hansen J, Nazarenko L, Luo Y (2002) Climate effects of black carbon aerosols in China and India. *Science* 297:2250–2253
- Menon S, Koch D, Beig G, Sahu S, Fasullo J, Orlikowski D (2010) Black carbon aerosols and the third polar ice cap. *Atmos Chem Phys* 10:4559–4571. <https://doi.org/10.5194/acp-10-4559-2010>
- Monahan EC (1986) The ocean as a source for atmospheric particles. In: Buat-Menard P (ed) *The role of air-sea exchange in geochemical cycling*. D. Reidel, Hingham, MA, pp 129–163

- Moorthy et al (1999) Aerosol climatology over India. 1-ISRO GBP MWR network and database. ISRO/GBP, SR-03-99
- Moorthy KK, Babu SS, Sunilkumar SV, Gupta PK, Gera BS (2004) Altitude profiles of aerosol BC, derived from aircraft measurements over an inland urban location in India. *Geophys Res Lett* 31:L22103. <https://doi.org/10.1029/2004gl021336>
- Moorthy KK, Satheesh SK, Babu SS, Dutt CBS (2008) Integrated Campaign for Aerosols, gases and Radiation Budget (ICARB): an overview. *J Earth Syst Sci* 117:243–262
- Moorthy KK, Babu SS, Manoj MR, Satheesh SK (2013a) Buildup of aerosols over the Indian region. *Geophys Res Lett* 40:1011–1014. <https://doi.org/10.1002/grl.50165>
- Moorthy KK, Beegum SN, Srivastava N, Satheesh SK, Chin M, Blond N, Babu SS, Singh S (2013b) Performance evaluation of chemistry transport models over India. *Atmos Environ* 71:210–225
- Morys M, Mims FM III, Hagerup S, Anderson SE, Backer A, Kia J, Walkup T (2001) Design, calibration and performance of Microtops II hand-held ozone monitor and sun photometer. *J Geophys Res* 106:14573–14582
- Myhre G, Stordal F, Restad K, Isaksen I (1998) Estimates of the direct radiative forcing due to sulfate and soot aerosols. *Tellus Ser B* 50:463–477
- Nair VS, Solmon F, Giorgi F, Mariotti L, Babu SS, Moorthy KK (2012) Simulation of South Asian aerosols for regional climate studies. *J Geophys Res* 117:D04209. <https://doi.org/10.1029/2011JD016711>
- Naja M, Bhardwaj P, Singh N, Kumar P, Kumar R, Ojha N, Sagar R, Satheesh SK, Moorthy KK, Kotamarthi VR (2016) High-frequency vertical profiling of meteorological parameters using AMF1 facility during RAWEX–GVAX at ARIES Nainital. *Curr Sci* 111(1):132–140. ISSN 0011-3891
- Omar AH, Winker DM, Vaughan MA, Hu Y, Trepte CR, Ferrare RA, Lee KP, Hostetler CA, Kittaka C, Rogers RR, Kuehn RE, Liu Z (2009) The CALIPSO automated aerosol classification and Lidar ratio selection algorithm. *J Atmos Ocean Technol* 26:1994–2014. <https://doi.org/10.1175/2009JTECHA1231.1>
- Pant P, Hegde P, Dumka UC, Sagar R, Satheesh SK, Moorthy KK, Saha A, Srivastava MK (2006) Aerosol characteristics at a high-altitude location in central Himalayas: optical properties and radiative forcing. *J Geophys Res* 111:D17206. <https://doi.org/10.1029/2005JD006768>
- Porch W, Chylek P, Dubey M, Massie S (2007) Trends in aerosol optical depth for cities in India. *Atmos Environ* 41:7524–7532. <https://doi.org/10.1016/j.atmosenv.2007.05.055>
- Prospero JM, Ginoux P, Torres O, Nicholson SE, Gill TE (2002) Environmental characterization of global sources of atmospheric soil dust identified with the Nimbus 7 Total ozone Mapping Spectrometer (TOMS) absorbing aerosol product. *Rev Geophys* 40:1002. <https://doi.org/10.1029/2000RG000095>
- Prospero JM, Charlson RJ, Mohnen B, Jaencke R, Delany AC, Mayers J, Zoller W, Rahn K (1983) The atmospheric aerosol system—an overview. *Rev Geophys* 21:1607–1629
- Pruppacher HR, Klett JD (1978) *Microphysics of clouds and precipitation*. D. Reidel Publishing Company, Holland
- Ramanathan V, Crutzen PJ, Kiehl JT, Rosenfeld D (2001a) Aerosols, climate and the hydrological cycle. *Science* 294:2119–2124
- Ramanathan V et al (2001b) Indian Ocean experiment: an integrated analysis of the climate forcing and effects of the great Indo-Asian haze. *J Geophys Res* 106:28371–28398
- Ramanathan V, Raman MV, Roberts G, Kim D, Corrigan C, Chung C, Winker D (2007) Warming trends in Asia amplified by brown cloud solar absorption. *Nature* 448:575–578. <https://doi.org/10.1038/nature06019>
- Sagar R, Kumar B, Dumka UC, Moorthy KK, Pant P (2004) Characteristics of aerosol optical depths over Manora Peak: a high altitude station in the central Himalayas. *J Geophys Res* 109:D06207. <https://doi.org/10.1029/2003JD003954>
- Satheesh SK, Ramanathan V (2000) Large differences in the tropical aerosol forcing at the top of the atmosphere and Earth's surface. *Nature* 405:60–63. <https://doi.org/10.1038/35011039>

- Satheesh SK et al (2008) Climate implications of large warming by elevated aerosol over India. *Geophys Res Lett* 35:L19809. <https://doi.org/10.1029/2008GL034944>
- Saxena P, Hildemann LM (1996) Water soluble organics in atmospheric particles: a critical review of the literature and application of thermodynamics to identify candidate compounds. *J Atmos Chem* 24:57–109
- Seinfeld JH et al (2004) ACE-Asia—regional climatic and atmospheric chemical effects of Asian dust and pollution. *Bull Am Meteorol Soc* 85(3):367–380
- Seinfeld JH, Pandis SN (1998) *Atmospheric chemistry and physics—from air pollution to climate change*. Wiley, New York, USA
- Sikka DR (1997) Desert climate and its dynamics. *Curr Sci India* 72:35–46
- Singh RP, Dey S, Tripathi SN, Tare V (2004) Variability of aerosol parameters over Kanpur, northern India. *J Geophys Res* 109:D23206. <https://doi.org/10.1029/2004JD004966>
- Skamarock WC et al (2008) A description of the advanced research WRF version 3. NCAR Tech. Note NCAR/TN-475+STR, Natl. Cent. for Atmos. Res., Boulder, CO, pp 125
- Smirnov A, Villevalde Y, O'Neill NT, Royer A, Tarussov A (1995) Aerosol optical depth over the oceans: analysis in terms of synoptic air mass types. *J Geophys Res* 16:639–650, 24513
- Srivastava AK, Ram K, Pant P, Hegde P, Joshi H (2012) Black carbon aerosols over Manora Peak in the Indian Himalayan foothills: implications for climate forcing. *Environ Res Lett* 7:014002. <https://doi.org/10.1088/1748-9326/7/1/014002>
- Stephens GL et al (2002) The CloudSat mission and the A-Train: a new dimension of space-based observations of clouds and precipitation. *Bull Am Meteorol Soc* 83:1771–1790
- Stohl A (1996) Trajectory statistics—a new method to establish source-receptor relationships of air pollutants and its application to the transport of particulate sulfate in Europe. *Atmos Environ* 30(4):579–587. [https://doi.org/10.1016/1352-2310\(95\)00314-2](https://doi.org/10.1016/1352-2310(95)00314-2)
- Stohl A (2006) Characteristics of atmospheric transport into the Arctic troposphere. *J Geophys Res* 111(11):D11306. <https://doi.org/10.1029/2005JD006888>
- Streets DG, Yan F, Chin M, Diehl T, Mahowald N, Schultz M, Wild M, Wu Y, Yu C (2009) Anthropogenic and natural contributions to regional trends in aerosol optical depth, 1980–2006. *J Geophys Res* 114:D00D18. <https://doi.org/10.1029/2008jd011624>
- Weingartner E, Saathof H, Schnaiter M, Streit N, Bitnar B, Baltensperger U (2003) Absorption of light by soot particles: determination of the absorption co-efficient by means of Aethalometers. *J Aerosol Sci* 34(10):1445–1463. [https://doi.org/10.1016/S0021-8502\(03\)00359-8](https://doi.org/10.1016/S0021-8502(03)00359-8)
- Whitby KT (1978) The physical characteristics of sulfur aerosols. *Atmos Environ* 12:135–159
- Winker DM, Vaughan MA, Omar AH, Hu Y, Powell KA, Liu Z, Hunt WH, Young SA (2009) Overview of the CALIPSO mission and CALIOP data processing algorithms. *J Atmos Ocean Technol* 26:2310–2323. <https://doi.org/10.1175/2009JTECHA1281.1>
- Young SA, Vaughan MA (2009) The retrieval of profiles of particulate extinction from Cloud Aerosol Lidar Infrared Pathfinder Satellite Observations (CALIPSO) data: algorithm description. *J Atmos Ocean Technol* 26:1105–1119. <https://doi.org/10.1175/2008JTECHA1221.1>
- Zhang J, Reid JS (2010) A decadal regional and global trend analysis of the aerosol optical depth using a data-assimilation grade over-water MODIS and Level 2 MISR aerosol products. *Atmos Chem Phys* 10(22):10949–10963. <https://doi.org/10.5194/acp-10-10949-2010>